

NEXAFS Investigation of the Mg-Pd nanoparticles before and after the Exposure to the Hydrogen Gas

**Satoshi Ogawa¹, Tsuyoshi Mizutani², Masahiro Ogawa³, Chihiro Yogi³,
Toshiaki Ohta³, Tomoko Yoshida⁴, Shinya Yagi⁴**

1) Department of Quantum Engineering, Graduate School of Engineering, Nagoya University, Furo-cho, Chikusa-ku, Nagoya, 464-8603, Japan

2) Department of Materials, Physics and Energy Engineering, Graduate School of Engineering, Nagoya University, Furo-cho, Chikusa-ku, Nagoya, 464-8603, Japan

3) The SR center, Ritsumeikan University, 1-1-1 Noji-Higashi, Kusatsu, Shiga, 525-8577, Japan

4) EcoTopia Science Institute, Nagoya University, Furo-cho, Chikusa-ku, Nagoya, 464-8603, Japan

Abstract

We have investigated the chemical state around the Mg and Pd atoms in the Mg-Pd nanoparticles by the Mg K- and Pd L₃-edges NEXAFS techniques without the air oxidation of the nanoparticles. NEXAFS analyses have revealed that the Mg-Pd nanoparticles possess metallic Mg and Pd states and the surface of the Mg-Pd nanoparticles is partly oxidized. Furthermore, both the Mg K- and Pd L₃-edges NEXAFS spectra imply that the Mg-Pd alloy phases are formed in the Mg-Pd nanoparticles. We have also investigated the variation of the chemical states around the Pd atom after the cycles of the exposure to the H₂ gas by the Pd L₃-edge NEXAFS. The Pd L₃-edge NEXAFS analysis has shown that the dissociation of the Mg-Pd alloy phases has been caused by the cycles of hydrogenation and dehydrogenation.

1. Introduction

The future energy system using hydrogen as energy carrier is expected as the alternative energy system to the current energy system. Hydrogen storage materials play important role as the storage chamber of the hydrogen. Magnesium (Mg) is attractive material for hydrogen (H) storage because MgH_2 achieves high hydrogen storage amount of 7.6 wt%. Furthermore, Mg is lightweight and inexpensive compared with other candidates of the hydrogen storage materials. There are two problems in application of Mg to the hydrogen storage system: both hydro-/dehydrogenation reactions of Mg require i) time scale of a few hours and ii) high temperature condition. These difficulties are attributed to low diffusion rate of hydrogen inside of Mg and low dissociation activity of H_2 molecule at Mg surface. The hydrogen diffusion kinetics inside of Mg is limited by the MgH_2 layer. The decrease of diffusion length is favorable for the complete of hydro-/dehydrogenation of Mg, i.e. nanomaterial of Mg such as Mg nanoparticle is superior to bulk materials [1, 2]. Moreover, addition of transition metal as catalyst is effective for improvement of dissociation activity of the H_2 molecule. The Mg thin film capped by palladium (Pd) layer can storage hydrogen at room temperature under 0.1 MPa of the H_2 gas within several tens of seconds [3]. The Pd layer can dissociate the H_2 molecule and also transport hydrogen to the Mg layer via the Mg-Pd alloy layer between the Mg and Pd layers. In this study, we have investigated the chemical state around the Mg and Pd atoms in the Mg-Pd nanoparticles by the near Mg K- and Pd L_3 -edges X-ray absorption fine structure (Mg K- and Pd L_3 -edges NEXAFS) techniques. The Mg-Pd nanoparticles consisted of the both Mg and Pd atoms have been fabricated by the gas evaporation method using He gas. The XAFS measurements have been carried out without the exposure to the air due to easy oxidizability of the Mg nanomaterials [4-6]. Furthermore, we have focused on the variation of the chemical state around the Pd atoms before and after the exposure to the H_2 gas.

.....

2. Experimental

Fabrication of the Mg-Pd nanoparticles

The Mg-Pd nanoparticles were fabricated by the gas evaporation method using He gas (purity: 99.99995 %) [7]. The rod shaped Mg and Pd wire were used as the evaporation sources. These sources equipped in the same evaporation chamber were evaporated simultaneously under the He gas atmosphere of 9 kPa. The Mg-Pd nanoparticles were formed by condensation of the Mg and Pd atoms in the He atmosphere and deposited on the Si(100) substrate. Fig. 1 shows the high-resolution transmission electron microscopy (HRTEM) image of the Mg-Pd nanoparticles deposited on the Cu micro-grid. The obvious

lattice fringes in Fig.1 represent that the Mg-Pd nanoparticles have the crystal structure. The size of Mg-Pd nanoparticles was evaluated by the atomic force microscopy (AFM). The AFM observation was carried out with noncontact mode under the atmospheric condition. The diameter of Mg-Pd nanoparticles has been evaluated by the height value of the AFM image because of high resolution in vertical direction of the AFM observation compared with horizontal one. The size distribution of Mg-Pd nanoparticles is shown in Fig. 1. The average diameter of Mg-Pd nanoparticles was evaluated to be 4.5 nm.

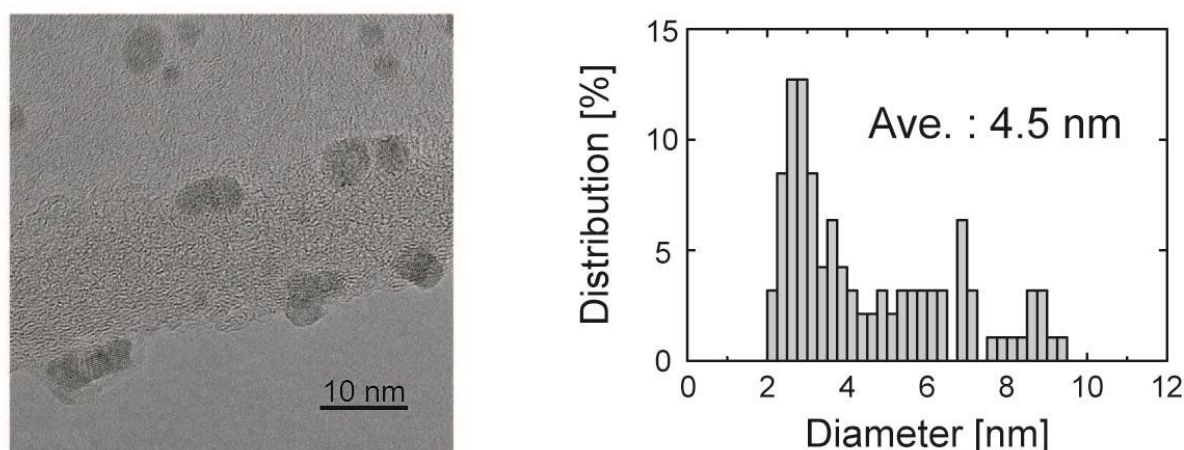


Fig. 1 HRTEM image (left side) and the size distribution of the Mg-Pd nanoparticles (right side).

Mg K- and Pd L₃-edges NEXAFS measurement

The Mg K- and Pd L₃-edges NEXAFS measurements using synchrotron radiation light source were carried out at BL-10 of the SR center in Ritsumeikan University [8, 9]. A Golovchenko-type double-crystal monochromator with beryl(10-10) crystal for Mg K-edge and Ge(111) for Pd L₃-edge was used for the selection of incident X-ray energy. NEXAFS spectra were obtained by total electron yield (TEY) method with the sample drain current under high vacuum condition ($\sim 1 \times 10^{-6}$ Pa). The incident X-ray energy for Mg K- and Pd L₃-edges NEXAFS measurements was calibrated with the first peaks of the NEXAFS spectra for MgO powder at 1309.3 eV and metallic Pd at 3174.9 eV, respectively. In the NEXAFS measurement, the chamber for fabrication of the Mg-Pd nanoparticles was connected to the XAFS chamber at the BL-10 in order to protect the Mg-Pd nanoparticles against the air oxidation.

After the NEXAFS measurement for as-fabricated samples, the exposure of the Mg-Pd nanoparticles to the H₂ gas has been carried out with the transfer vessel [10]. The transfer

vessel is composed of the gate valve and the small sample chamber. The Mg-Pd nanoparticle sample was transferred to the sample chamber under the high vacuum and the sample chamber was separated from the fabrication chamber by closing of the gate valve. After removal of the transfer vessel from the vacuum chamber, the transfer vessel was connected to the H₂ gas supply line and fulfilled by H₂ gas of 0.2 MPa, then the transfer vessel was evacuated to vacuum after the exposure to the H₂ gas for 5 minutes (1 cycle of the exposure to the H₂ gas).

.....

3. Results and Discussion

The Mg K-edge NEXAFS spectrum of the Mg-Pd nanoparticles is shown in Fig. 2. Mg K-edge NEXAFS represents the chemical state around the Mg atoms inside of the Mg-Pd nanoparticles. The shoulder structure around 1304 eV can be seen clearly in the NEXAFS spectrum of the Mg-Pd nanoparticles. Since this shoulder structure is finger print of the chemical state of the metallic Mg in Mg K-edge NEXAFS [6], Mg-Pd nanoparticles partly consist of the metallic Mg. The peak structure associated with the chemical state of MgO around 1309 eV can be also seen in the spectrum of the Mg-Pd nanoparticles. It seems that the surface of the Mg-Pd nanoparticles is oxidized by the residual gas in the vacuum chamber despite of the high vacuum condition.

If the chemical states around Mg atom in the Mg-Pd nanoparticles only consist of the metallic Mg and MgO, we can simulate the NEXAFS spectrum of the Mg-Pd nanoparticles by linear combination of the spectrum for the metallic Mg and MgO. The simulation of the NEXAFS spectrum of the Mg-Pd nanoparticles is shown in Fig. 2. The each fractions of the spectra for metallic Mg and MgO were 0.61 and 0.14, respectively. The features of NEXAFS spectra of the metallic Mg

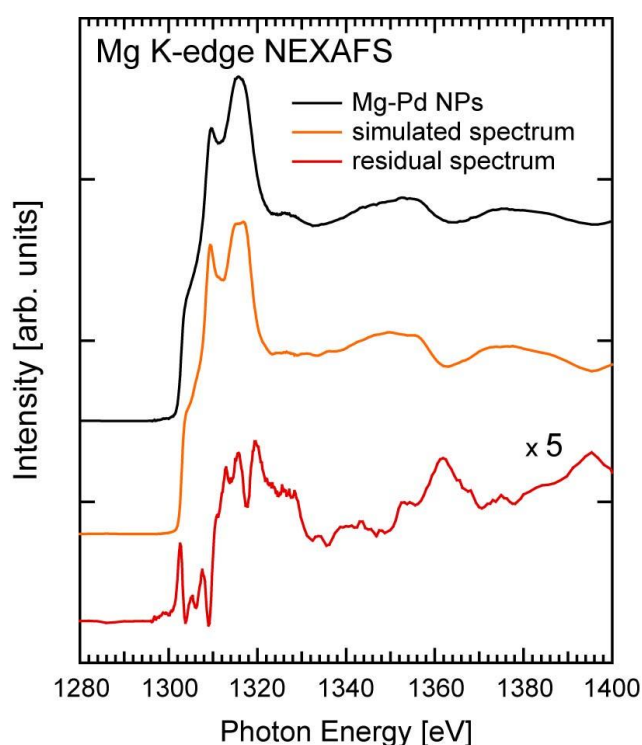


Fig. 2 Mg K-edge NEXAFS spectrum for the Mg-Pd nanoparticles (black solid line). The simulated spectrum (orange solid line) is composed of 0.61 and 0.14 times of standard spectrum for metallic Mg and MgO, respectively.

and the MgO are characterized by the shoulder structure at 1304 eV for the metallic Mg and the peak structure at 1309 eV for MgO, respectively. Hence, the simulation has been done to vanish the main features of each chemical states. It is difficult to simulate completely the NEXAFS spectrum of the Mg-Pd nanoparticles by the linear combination of the spectra for the metallic Mg and the MgO. The residual spectrum is shown at downside in Fig. 2. The features of the residual spectrum is not similar to that of NEXAFS spectrum for the oxidation products ($\text{Mg}(\text{OH})_2$, MgCO_3 , ...). It seems that the residual spectrum represents the interaction with the neighboring Pd atoms, i.e. the chemical state of the Mg-Pd alloy.

Pd L_3 -edges NEXAFS is suitable for identification of the chemical state of Pd due to the sensitivity of the main peak position to the chemical environment around Pd atom [11]. Fig. 3 shows the Pd L_3 -edges NEXAFS spectra of the Mg-Pd nanoparticles and metallic Pd. The energy shift of main peak position of the NEXAFS spectrum for the Mg-Pd nanoparticles toward higher energy side compared with that of metallic Pd implies the charge transfer from Pd atom to the other atoms. The main peak position of the spectrum for the Mg-Pd nanoparticles dose not correspond to that of PdO [11]. It is considered that the valence electrons of the Pd atom are transfered toward Mg atom and Mg-Pd bond is

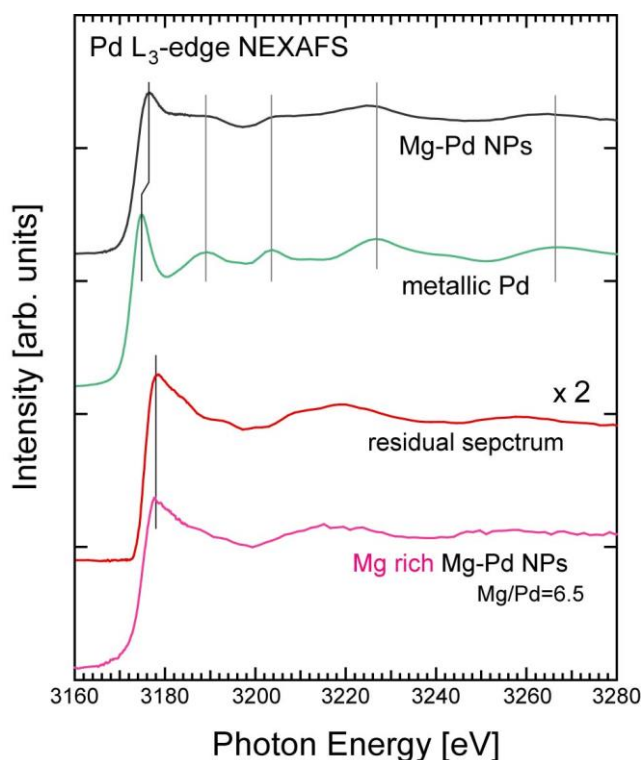


Fig. 3 Pd L_3 -edge NEXAFS spectrum for the as-fabricated Mg-Pd nanoparticles. The NEXAFS spectrum for the metallic Pd is shown as the standard spectrum. The residual spectrum has been obtained after the subtraction of 0.50 times of the spectrum for the metallic Pd from that of the Mg-Pd nanoparticles.

formed. On the other hand, the peak structures in the energy range of 3180-3280 eV correspond to those of metallic Pd. These results represent the existence of the chemical state of metallic Pd in the Mg-Pd nanoparticles in addition to Mg-Pd alloy state.

We can obtain the NEXAFS features of Mg-Pd alloy state as the residual spectrum after the subtraction of the NEXAFS spectrum for the metallic Pd from that of the Mg-Pd nanoparticles. The NEXAFS features for the Mg-Pd alloy state are shown in Fig. 3 as the residual spectrum. The subtractions have been done to vanish the main feature of the NEXAFS spectrum for the metallic state of Pd (3174.9 eV). Pd L₃-edge NEXAFS spectrum of Mg rich Mg-Pd nanoparticles is also shown in Fig. 6 as the reference spectrum. The atomic ratio of Mg/Pd for the Mg rich Mg-Pd nanoparticles has been estimated to be 6.5 by the X-ray fluorescence analysis using the synchrotron radiation. The consistence of the shape of the NEXAFS features between the residual spectrum and the Mg rich Mg-Pd nanoparticles represents that the Mg-Pd nanoparticles possess the Mg rich Mg-Pd alloy phase before the exposure to the H₂ gas.

The variation of the chemical state of the Mg-Pd nanoparticles after the cycles of the exposure to the H₂ gas has been investigated by the Pd L₃-edges NEXAFS. Fig. 4 shows the Pd L₃-edge NEXAFS spectra of the Mg-Pd nanoparticles after the cycles of the exposure to the H₂ gas. The main peak position of the NEXAFS spectrum for the Mg-Pd nanoparticles

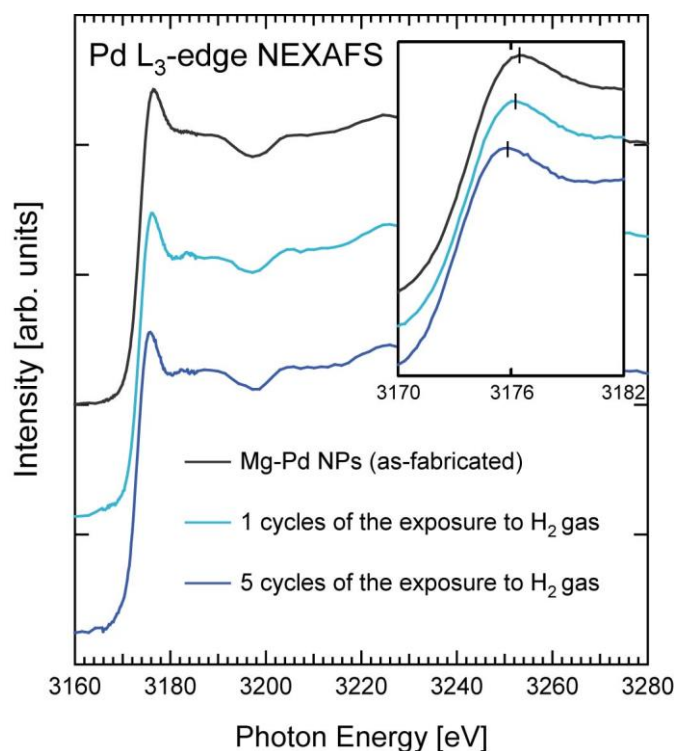


Fig. 4 The variation of the Pd L₃-edge NEXAFS spectra for the Mg-Pd nanoparticles before and after the exposure to the H₂ gas.

shifts slightly toward low energy side as the cycles of exposure to the H₂ gas (inset figure in Fig. 4), although the shape of the NEXAFS spectrum does not vary significantly. These continuous peak shifts imply the increase of the fraction of metallic Pd in the Mg-Pd nanoparticles by hydrogenation and dehydrogenation.

In order to investigate the variation of the chemical state of the Mg-Pd alloy before and after the exposure to the H₂ gas, the NEXAFS spectrum for the metallic Pd has been subtracted from the each spectra in Fig. 4 and the residual spectra after the subtraction are shown in Fig. 5. The residual spectra in Fig. 5 represent the Mg-Pd alloy phase in the Mg-Pd nanoparticles. In addition to residual spectra, Pd L₃-edges NEXAFS spectra of Mg rich and Pd rich Mg-Pd nanoparticles are also shown in Fig. 6 as the reference spectra. All spectra are normalized with respect to heights of the edge jump. Comparison between the Mg rich and Pd rich Mg-Pd nanoparticles reveals that the peak features at 3177.6 eV and 3181.2 eV are associated with Mg rich and Pd rich Mg-Pd alloy phases, respectively. The variation of the chemical state of the Mg-Pd alloy phases is clearly seen in relative intensity between the peak features at 3177.6 eV and 3181.2 eV. The relative intensity of the peak at 3177.6 eV is higher than the that of the peak at 3181.2 eV in the spectrum for the Mg-Pd

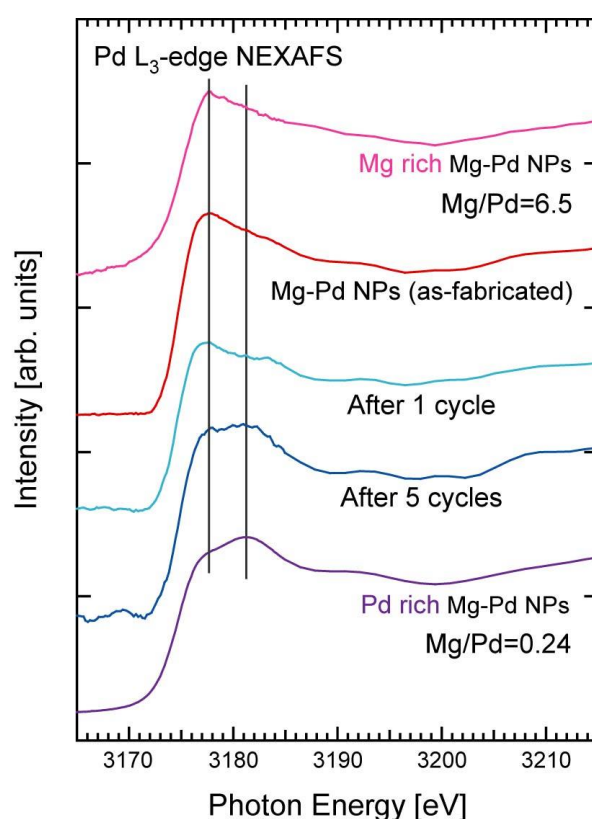


Fig. 5 The variation of the Pd L₃-edge NEXAFS spectra for the Mg-Pd alloy states before and after the exposure to the H₂ gas. The NEXAFS spectra for the Mg-Pd alloy states have been obtained after the subtraction of the spectrum for the metallic Pd from the spectra in Fig. 4.

nanoparticles before the exposure to the H₂ gas. This relativity of the intensities between the peaks at 3177.6 eV and 3181.2 eV varies gradually as the cycles of the exposure to the H₂ gas. Finally, the relative intensities of the two peaks are comparable in the spectrum for the Mg-Pd nanoparticles after 5 cycles of the exposure to the H₂ gas.

These results indicate that the cycles of the hydrogenation and dehydrogenation of Mg atoms cause the dissociation of the Mg-Pd alloy phases. The Mg-Pd alloy phases improve the diffusion of the hydrogen atoms between the Mg and Pd phases [3]. We speculate that when the hydrogen atoms penetrate into the alloy phases, the Mg-Pd bondings in the alloy phases are broken due to the high affinity between H and Mg atoms. Consequently, the hydrogen atoms settle inside the Mg-Pd alloy phases as MgH₂ and the excess Pd atoms form the metallic Pd phases or the Pd rich Mg-Pd alloy phases.

.....

4. Conclusions

The nanoparticles composed of the Mg and Pd atoms (Mg-Pd nanoparticles) have been fabricated by the simultaneous evaporation of the Mg and Pd sources under the He atmosphere. The average size of the Mg-Pd nanoparticles evaluated by the AFM observation is 4.5 nm. The Mg K- and Pd L₃-edges NEXAFS measurements have been carried out with the synchrotron radiation without the exposure to the air in order to investigate the chemical states around the Mg and Pd atoms in the Mg-Pd nanoparticles. The Mg K- and Pd L₃-edges NEXAFS investigations represent that the large part of Mg-Pd nanoparticles consist of metallic Mg and Pd states. Both the Mg K- and Pd L₃-edges NEXAFS spectra indicate the formation of Mg-Pd alloy phases in the Mg-Pd nanoparticles. The variation of the chemical state of the Mg-Pd nanoparticles before and after the cycle of the exposure to the H₂ gas has been investigated by the Pd L₃-edge NEXAFS measurements. It is apparent that the Mg rich Mg-Pd alloy phases dissociate with the cycle of the hydro-dehydrogenation and the domain of metallic Pd phases increase gradually.

Acknowledgement

The authors are grateful for the financial support of JSPS Research Fellowship for Young Scientists (No. 236237) and Knowledge Cluster II in Aichi/Nagoya area. This work was performed under the approval of Ritsumeikan University SR center Program Advisory Committee. The authors also thank Dr. Junko Matsuda, Dr. Hiroaki Nameki, Dr. Koji Nakanishi and Mr. Yoshitada Abe for their helpful technical support.

References

- (1) R.W.P. Wagemans, J.H. van Lenthe, P.E. de Jongh, A.J. van Dillen and K.P. de Jong, *J. Am. Chem. Soc.* **127**, 47, 16675-16680 (2005).
- (2) K.J. Jeon, H.R. Moon, A.M. Ruminski, B. Jiang, C. Kisielowski, R. Bardhan and J.J. Urban, *Nature Materials* **10**, 286-290 (2011).
- (3) K. Yoshimura, Y. Yamada, M. Okada, *Surf. Sci.* **566-568**, 751-754 (2004).
- (4) S. Ogawa, H. Niwa, T. Nomoto and S. Yagi, *e-J. Surf. Sci. Nanotech.* **8**, 246-249 (2010).
- (5) S. Ogawa, H. Niwa, K. Nakanishi, T. Ohta and S. Yagi, *J. Surf. Anal.* **17**, 319-323 (2011).
- (6) S. Ogawa, S. Murakami, K. Shirai, K. Nakanishi, C. Tsukada, T. Ohta and S. Yagi, *e-J. Surf. Sci. Nanotech.* **9**, 315-321 (2011).
- (7) S. Yagi, H. Sumida, K. Miura, T. Nomoto, K. Soda, G. Kutluk, H. Namatame and S. Taniguchi, *e-J. Surf. Sci. Nanotech.* **4**, 258-262 (2006).
- (8) K. Nakanishi, S. Yagi and T. Ohta, *AIP Conf. Proc.* **1234**, 931 (2010).
- (9) K. Nakanishi, T. Ohta, *Surf. Interface Anal.* **44**, 6, 784 (2012).
- (10) K. Nakanishi, S. Yagi, and T. Ohta, *IEEJ Trans. EIS* **130**, 10, 1762-1767 (2010).
- (11) Z. Liu, K. Handa, K. Kaibuchi, Y. Tanaka, J. Kawai, *Spectrochim. Acta Part B* **59**, 901-94 (2004).